Electronic Supplementary Material (ESI) for Nanoscale.
This journal is © The Royal Society of Chemistry 2021

A quantitative model for a nanoscale switch accurately predicts thermal actuation behavior

Electronic Supplementary Information

Kyle Crocker,[a] Joshua Johnson,[bc] Wolfgang Pfeifer,[ad] Carlos Castro,[bd] and Ralf Bundschuh*[abefg]

S1 Salt corrected base pairing parameters

We calculate the salt corrected base pairing parameter values using the melting temperature correction

$$\frac{1}{T_m(\mathrm{Mg}^{2+})} = \frac{1}{T_m(1\ \mathrm{M\ Na}^{+})} + a + b\ln[\mathrm{Mg}^{2+}] + f_{GC}(c + d\ln[\mathrm{Mg}^{2+}]) + \frac{1}{2(N_{bp}-1)}\left\{e + f\ln[\mathrm{Mg}^{2+}] + g(\ln[\mathrm{Mg}^{2+}])^2\right\} \quad (11)$$

given by Owczarzy et al.[50], where a, b, c, d, e, f, and g are experimentally determined constants. We use the magnesium salt correction since our and Johnson *et al.*'s experiments are performed in the presence of 11.5 mM free magnesium. Since we care about the change in base pairing energy for a generic internal base, we ignore edge effects by taking the limit as N_{bp} approaches infinity. Furthermore, our sequences consist solely of A's and T's, so the fraction of G and C bases $f_{GC} = 0$. Thus the melting temperature in our case is given by

$$\frac{1}{T_m(\mathrm{Mg}^{2+})} = \frac{1}{T_m(1\ \mathrm{M\ Na}^{+})} + \left(3.92 - 0.911\ln[0.0115]\right)\times 10^{-5}\,\frac{1}{K} \quad (12)$$

where we have substituted the appropriate constants for a and b.

Since the melting temperature is the temperature at which the base pairing energy change is 0, we can write the melting temperature in terms of the base pairing entropy and enthalpy change as

$$T_m = \Delta H_{bp}/\Delta S_{bp}. \quad (13)$$

Assuming that salt concentration only impacts base pairing entropy[47,51,52], the corrected base pairing entropy change $\Delta S_{bp,c}$ is given by

$$\Delta S_{bp,c} = \frac{\Delta H_{bp}}{T_m(\mathrm{Mg}^{2+})} \quad (14)$$

with $T_m(\mathrm{Mg}^{2+})$ from Eq. (12).

S2 Modeling the effect of fraying or sliding

In order to disentangle the effects of fraying and sliding of the DNA duplexes between the overhangs and the DNA strands on the AuNP, we use alternative models that exclude each of them separately, or exclude both effects. Fraying and sliding enter the original model via the multiplicities in Eq. (5). We thus here provide alternative versions of Eq. (5) for the three different cases that exclude fraying and/or sliding.

S2.1 Model with no fraying or sliding

In order to exclude fraying and sliding, Eq. (5) becomes

$$Z_{\mathrm{S},j} = \exp\left[-\frac{\Delta G_{\mathrm{term}} + N_{\mathrm{S},j}\Delta G_{bp}}{k_B T}\right], \quad (15)$$

since there is now only a single state allowed with free energy $\Delta G_{\mathrm{term}} + N_{\mathrm{S},j}\Delta G_s$.

S2.2 Model with no fraying

In order to exclude only fraying, Eq. (5) becomes

$$Z_{\mathrm{S},j} = (|N_{\mathrm{T}} - N_{\mathrm{A},j}| + 1)\exp\left[-\frac{\Delta G_{\mathrm{term}} + N_{\mathrm{S},j}\Delta G_{bp}}{k_B T}\right], \quad (16)$$

where the prefactor is simply the number of positions available to completely paired strands.

S2.3 Model with no sliding

In order to exclude only sliding, Eq. (5) becomes

$$Z_{\mathrm{S},j} = \sum_{i=1}^{N_{\mathrm{S},j}} (N_{\mathrm{S},j} - i + 1)\exp\left[-\frac{\Delta G_{\mathrm{term}} + i\Delta G_{bp}}{k_B T}\right], \quad (17)$$

where the sum is over the number of possible base paired stacks, and the prefactor gives the multiplicity of each of these stacks.

* Corresponding author.
[a] Department of Physics, The Ohio State University, Columbus, OH 43210, USA. E-mail: bundschuh@mps.ohio-state.edu
[b] Interdisciplinary Biophysics Graduate Program, The Ohio State University, Columbus, OH 43210, USA.
[c] Department of Chemistry, Imperial College London, Molecular Sciences Research Hub, 80 Wood Lane, London W12 0BZ, UK.
[d] Department of Mechanical and Aerospace Engineering, The Ohio State University, Columbus, OH 43210, USA.
[e] Department of Chemistry and Biochemistry, The Ohio State University, Columbus, OH 43210, USA.
[f] Division of Hematology, Department of Internal Medicine, The Ohio State University, Columbus, OH 43210, USA.
[g] Center for RNA Biology, The Ohio State University, Columbus, OH 43210, USA.

S3 Supplemental tables

Table S1 Fixed base pairing parameter fit results (used in Fig. S2) in units of kJ/mol for enthalpies and kJ/(mol K) for entropies. Values without errors are fixed.

Data fit	ΔH_{cl}	ΔS_{cl}	ΔH_{bp}	ΔS_{bp}	ΔS_b
Enthalpy fixed	0 ± 2.0	-0.025 ± 0.006	-33.1	-0.0988 ± 0.0001	0.0429 ± 0.0008
Both fixed	0 ± 2.5	-0.019 ± 0.008	-33.1	-0.0955	0.0620 ± 0.0006

Table S2 Melt and anneal only parameters (used in Fig. S5 in units of kJ/mol for enthalpies and kJ/(mol K) for entropies.

Data fit	ΔH_{cl}	ΔS_{cl}	ΔH_{bp}	ΔS_{bp}	ΔS_b
Melt	0 ± 15	-0.038 ± 0.048	-38.1 ± 1.7	-0.114 ± 0.005	0.0369 ± 0.0007
Anneal	0 ± 13	-0.02 ± 0.04	-37.7 ± 1.6	-0.112 ± 0.005	0.060 ± 0.002

Table S3 No fraying and no sliding fit parameters in units of kJ/mol for enthalpies and kJ/(mol K) for entropies.

Model	ΔH_{cl}	ΔS_{cl}	ΔH_{bp}	ΔS_{bp}	ΔS_b
No slide or fray	0 ± 12	-0.02 ± 0.04	-28.7 ± 1.2	-0.085 ± 0.004	0.014 ± 0.001
No fray	0 ± 12	-0.02 ± 0.04	-28.7 ± 1.2	-0.084 ± 0.004	0.041 ± 0.001
No slide	0 ± 9.5	-0.02 ± 0.03	-36.0 ± 1.2	-0.108 ± 0.004	0.0204 ± 0.0009

Table S4 *VarS* fit parameter values: Model parameters used for curves shown in Fig. S8 in units of kJ/mol for enthalpies and kJ/(mol K) for entropies.

ΔH_{cl}	ΔS_{cl}	ΔH_{bp}	ΔS_{bp}	$\Delta S_{b,1}$	$\Delta S_{b,2}$	$\Delta S_{b,3}$
4.3 ± 0.3	-0.02	-33.7 ± 0.22	-0.1018 ± 0.0007	-0.05	-0.01	-0.05

S4 Supplemental figures

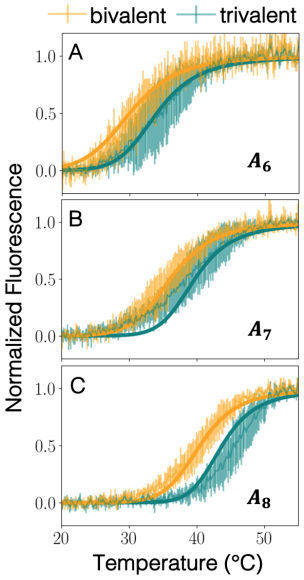

Fig. S1 Direct comparison of bivalent and trivalent actuation curves. The experimental data (thin lines) and model fits (thick lines) are identical to the ones shown in Fig. 3 but rather than separating the data by valency, each panel shows the bivalent (orange) and the trivalent (turquoise) case for (A) 6 base poly-A overhangs, (B) 7 base poly-A overhangs, and (C) 8 base poly-A overhangs.

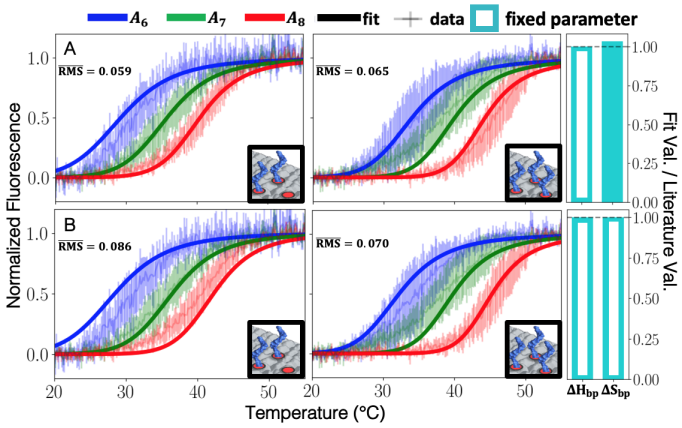

Fig. S2 Fits of the model described in section 2.3 with base pairing entropy and/or enthalpy fixed at literature values. In (A), base pairing enthalpy ΔH_{bp} is fixed at the SantaLucia expected value, and in (B) both the base pairing enthalpy and the salt corrected base pairing entropy ΔS_{bp} are fixed. In both cases, the model is fit to bivalent and trivalent data simultaneously. Each panel contains the average root mean squared difference ($\overline{\text{RMS}}$) between the model and the average of the experimental data. The rightmost column shows the ratio between the fit base pairing parameter values and the salt corrected expected base pairing parameter values given by Eq. (14). Since the outlined bars are fixed to the expected values, they have an actual to expected value ratio of 1. Fit parameters are given in Table S1.

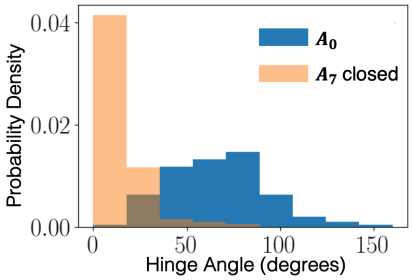

Fig. S3 Comparison between the opening angle distributions of a free nano-hinge (labelled A_0 to indicate that there are no bottom arm overhangs), and a closed trivalent nano-hinge with 7 base overhangs (labelled A_7). The relative entropy of the two distributions is ≈ -0.02 kJ / mol K. Data previously published by Johnson *et al.*[23].

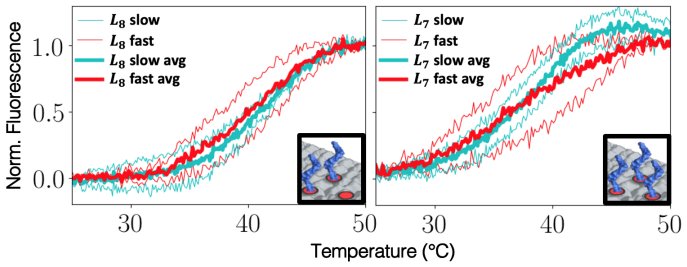

Fig. S4 Comparison of melting and annealing curves for varied rates using linker DNA instead of AuNPs. These experiments are similar to those with DNA nano-hinges containing AuNP, except that we add a duplex in place of the AuNP that binds to top and bottom overhangs that is the same size as the AuNP. These duplexes have poly-T single-stranded portions on the ends that mimic the single stranded poly-Ts that normally coat the AuNP. In particular, fabrication included hinges with 10 fold excess of linkers (200 nM) using the same folding protocol as for all other hinges. The left panel shows melting and annealing curves for two linkers annealing to 8 base overhangs, while the right panel shows melting and annealing curves for three linkers annealing to 7 base overhangs. For the red curves the temperature is changed at a rate of $2°C/min$, while for the green curves the temperature is changed at a rate of $0.2°C/min$. The thin lines show the individual melting and annealing curves while the thick lines indicate the averages of melting and annealing.

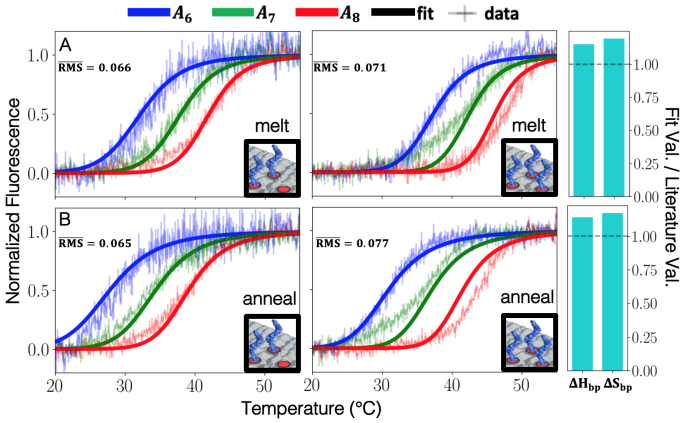

Fig. S5 Model described in section 2.3 fit to experimental datasets containing only melting (A) and only annealing (B) data. In both cases, the model is fit to bivalent and trivalent data simultaneously. Each panel contains the root mean squared difference ($\overline{RMS}$) between the model and the average of the experimental data. The rightmost column shows the ratio between the fit base pairing parameter values and the expected base pairing parameter values[47]. Fit values given in Table S2.

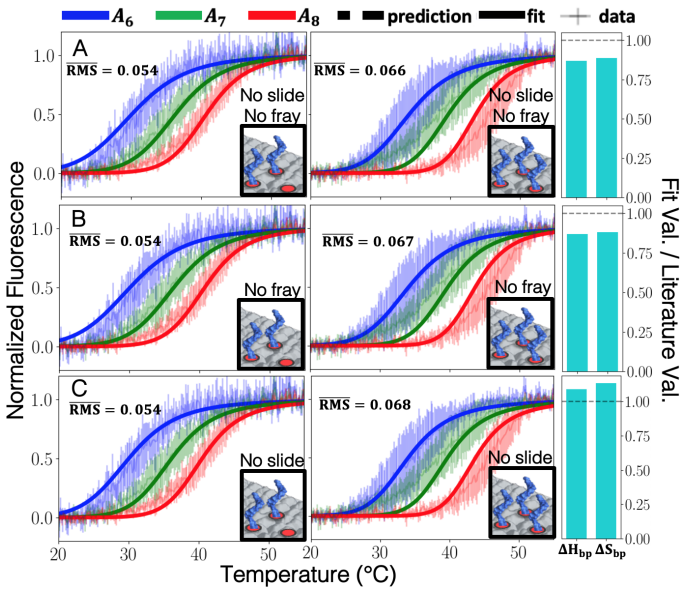

Fig. S6 Model described in section 2.3 with exclusion of fraying and/or sliding fit to experimental bivalent and trivalent data simultaneously. In row (A), both fraying and sliding are disallowed. In row (B), sliding is allowed, but fraying is disallowed. In row (C), fraying is allowed, but sliding is disallowed. Each panel contains the average root mean squared difference ($\overline{RMS}$) between the model and the average of the experimental data. The rightmost column shows the ratio between the fit base pairing parameter values and the expected base pairing parameter values[47].

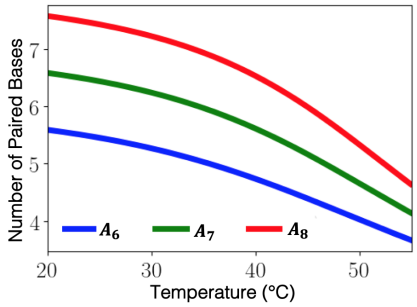

Fig. S7 Average paired bases for a connection of 6, 7, and 8 polyA bases calculated via Eq. (9) using parameters given in Table 1

.

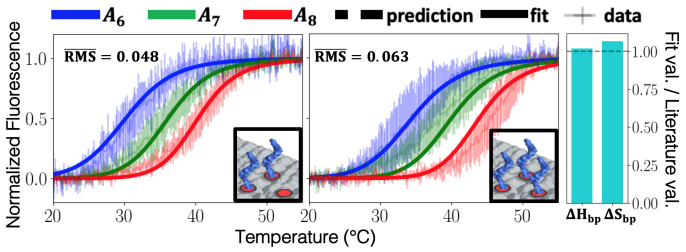

Fig. S8 *varS* model (described in section 3.7) fit to experimental data with ΔS_{cl}, $\Delta S_{b,1}$, $\Delta S_{b,2}$, and $\Delta S_{b,3}$ set to -0.02 , -0.05, -0.01, and -0.05 kJ/(mol K), respectively. The model (bold lines) is fit to bivalent and trivalent data simultaneously, with a bivalent comparison shown in the leftmost panel and a trivalent comparison shown in the middle panel. Each panel contains the averaged root mean squared difference ($\overline{\text{RMS}}$) between the model and the average of the experimental data. In particular, $\overline{\text{RMS}}$ is the average over the RMS differences for each curve shown in the panel. The rightmost column shows the ratio between the fit base pairing parameter values and the expected base pairing parameter values from the literature[47].

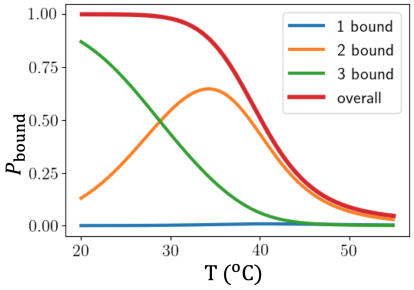

Fig. S9 Probability that 1, 2, or 3 overhang connections are bound for a trivalent 7 base nano-hinge as a function of temperature. Also shown in the overall probability that the nano-hinge is closed.

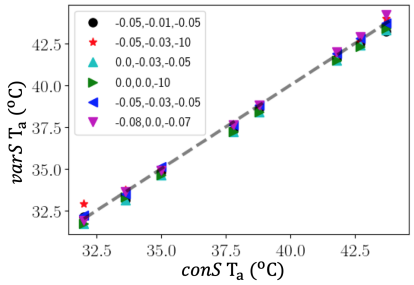

Fig. S10 Predictions are robust with respect to changes between the *varS* and *conS* models as well as different choices of *varS* parameters. Shown is a comparison of predicted actuation temperatures for the *conS* model on the x axis and the *varS* model on the y axis with various choices of ($\Delta S_{b,1}$, $\Delta S_{b,2}$, $\Delta S_{b,3}$) spread across the near-optimal volume. These choices are distinguished by symbols with values indicated in the legend in units of kJ / (mol K). The dashed line shows *varS* T_a = *conS* T_a to guide the eye.

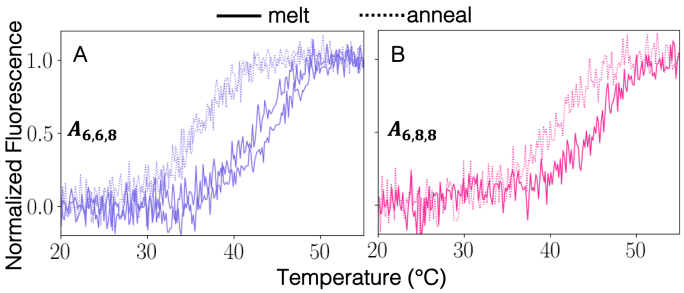

Fig. S11 Comparison of melting and annealing curves for mixed hinges. The left panel shows melting (solid) and annealing (dotted) curves for two experimental replicates of a nano-hinge with two 6-base overhangs and one 8-base overhang, and the right panel shows melting (solid) and annealing (dotted) curves for one experimental replicate of a nano-hinge with one 6-base overhang and two 8-base overhangs.